

Christoph Münkel \*  
Vaisala GmbH, Hamburg, Germany

Reijo Roininen  
Vaisala Oyj, Helsinki, Finland

## 1. INTRODUCTION





The vertical temperature and moisture distribution affect the layering of the atmospheric boundary layer and the existence of inversions within this layer or on the top of it. These layers have a strong influence on the development of episodes of high concentrations of air pollutants which might be harmful to people and ecosystems. The height of the mixing layer is defined as the height up to which due to the thermal structure of the boundary layer vertical dispersion by turbulent mixing of air pollutants takes place. Most of the aerosol particles in an atmospheric column are usually confined to atmospheric layers below this height, the knowledge on the mixing layer height can thus be employed to convert column-mean optical depths measured from satellites into near-surface air quality information.

Since several years, eye-safe lidar ceilometers are used for boundary layer monitoring. Emeis (2008) summarizes the methods used to derive aerosol layer heights from backscatter profiles and gives references to related publications. Comparison to temperature, humidity, and wind profiles reported by RASS, sodar, radio soundings, and weather mast in-situ sensors has confirmed their ability to detect convective or residual layers reaching up to heights exceeding 2500 m (Emeis (2009), Haman (2010), Münkel (2007), Münkel (2008)). Even more important for air quality applications is their near-range performance and the precise assessment of inversion layers and nocturnal stable layers below 200 m (Münkel, 2009). This was one of the reasons to apply a single lens optical design for the Vaisala Ceilometer CL31 (Münkel, 2008). This instrument has been chosen as standard cloud height indicator for the Automated Surface Observing System of the National Weather Service (Poyer, 2008).

## 2. VAISALA CEILOMETERS

Table 1 lists basic information about the standard ceilometer models manufactured by the company Vaisala. Only the CT12K uses a two lens optical setup; the one lens system of CT25K, CL31, and CL51 provides nearly full overlap of the transmitter and the

receiver field-of-view at distances below 30 m and thus improves their ability to investigate low inversion layers.

	CT12K	CT25K	CL31	CL51
Cloud reporting range	3800 m	7500 m	7500 m	13000 m
Manufactured	1987 - 1996	1995 - 2006	since 2005	since 2010
Installed base	2000	2600	2000	
				

**Table 1:** Vaisala ceilometers.

A detailed description of the CL31 ceilometer is given by Münkel (2008). The latest model, the CL51, is equipped with a larger lens and a more powerful laser transmitter module. These improvements increase cloud reporting range and signal-to-noise ratio, still also the CL51 is an eye-safe instrument with eye-safety class 1M.

## 3. METHOD

### 3.1 Gradient method

A widely applied approach to identify the vertical extent of aerosol layers within the planetary boundary layer is the gradient method that searches the range and overlap corrected attenuated backscatter profile for local gradient minima. For details see e.g. Münkel (2007). Its application to ceilometer data involves averaging in time and range.

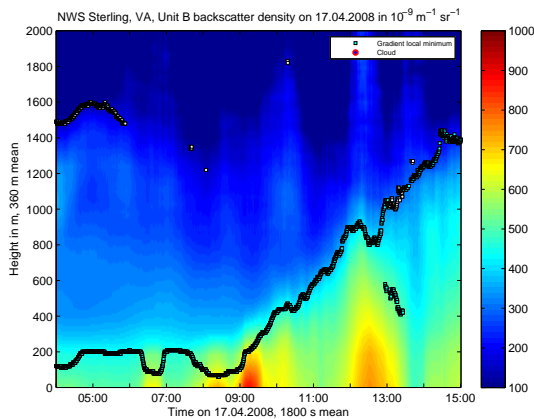
The CL31 and CL51 recommended report interval for aerosol investigation is 16 s; profile range resolution is 10 m. Applying 1800 s and 360 m time and height sliding averaging reveals local gradient minima within the profiles and thus information about aerosol layers.

Figure 1 shows such averaged profiles for a cloudless day. A nocturnal stable layer is visible until 09:00 local time; the evolution of a convective layer rising from 200 m to 1400 m can be followed from 09:00 to 15:00. During the first two hours of the graph a

---

\* Corresponding author address:  
Christoph Münkel, Vaisala GmbH,  
Schnackenburgallee 41d, 22525 Hamburg, Germany;  
e-mail: [christoph.muenkel@vaisala.com](mailto:christoph.muenkel@vaisala.com)

second gradient local minimum marks a residual layer at a height of 1500 m.



**Figure 1:** Density plot of overlap and range corrected ceilometer backscatter profiles recorded at the National Weather Service (NWS) test site Sterling, VA operated by the NWS Sterling Field Support Center on April 17, 2008. Fixed sliding averaging parameters are sufficient to reveal nocturnal stable, convective, and residual aerosol layers.

In Figure 2 backscatter profiles from a common day with rain and clouds are treated with the same gradient method parameters. Obviously the result is not very trustworthy and calls for a more sophisticated treatment. The following section describes the steps suggested to turn this standard gradient method into a robust algorithm that is able to identify situations when precipitation or fog prevents the detection of boundary layer height, and does not use high backscatter from preceding clouds for profile averaging.

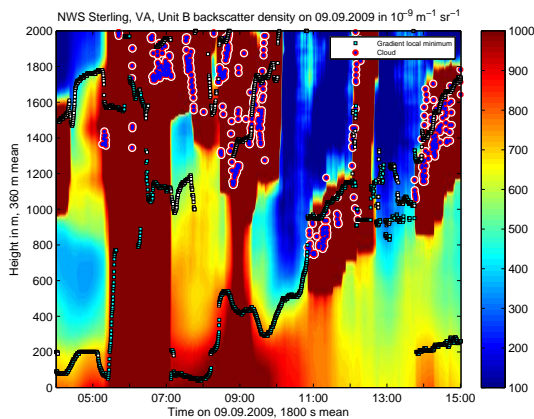


**Figure 2:** Density plot of overlap and range corrected ceilometer backscatter profiles recorded at the NWS test site Sterling, VA on September 9, 2009. On this common day with rain and clouds, applying the fixed sliding averaging parameters from Figure 1 does not reveal aerosol layers in a satisfactory way.

### 3.2 Steps towards an enhanced gradient method

The first step towards a robust all weather algorithm is a better data visualization. Large areas of Figure 2 show attenuated backscatter larger than  $10^{-6} \text{ m}^{-1} \text{ sr}^{-1}$ . Applying a logarithmic scaling covering the range  $50 \cdot 10^{-9} \text{ m}^{-1} \text{ sr}^{-1} - 20 \cdot 10^{-6} \text{ m}^{-1} \text{ sr}^{-1}$  helps to distinguish aerosol regions from clouds and precipitation (Figure 3).

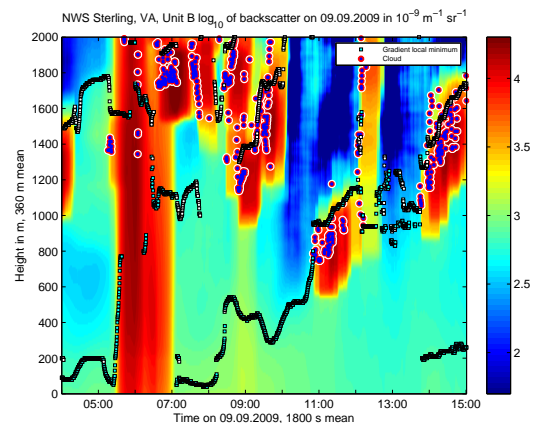


**Figure 3:** Logarithmic scaling applied to Figure 2 eases recognition of clouds and precipitation.

In Figure 3, the large backscatter values from the single 1300 m cloud at 09:40 are still visible half an hour later when no cloud was detected in that range. High backscatter from clouds and precipitation should therefore not be used in the averaging process. The result of applying this filter is shown in Figure 4. It reveals that there was no more precipitation after 06:30 and allows a better view on aerosol backscatter from the vicinity of clouds. Reporting of gradient minima is not done during the precipitation event.

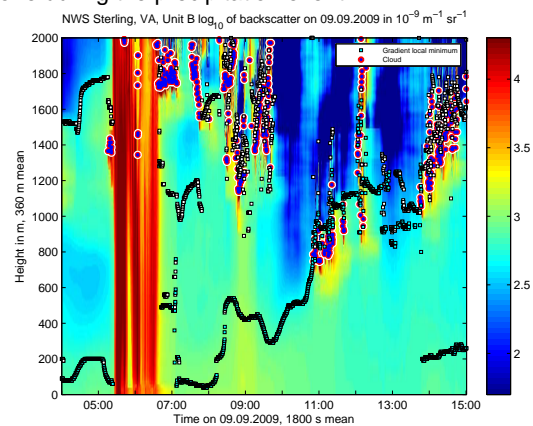


**Figure 4:** Result of the application of a cloud and precipitation filter to the data shown in Figure 3. This filter prevents the use of large backscatter values from hydrometeors for aerosol profile averaging.

Long averaging intervals help preventing false gradient minima hits generated by signal noise. On the other hand, this approach reduces the ability of the

algorithm to respond to short scale signal fluctuations in space and time. Signal noise amount is depending on range and time of the day. Figure 5 introduces variable averaging parameters that enable a much better view on a stable nocturnal layer at a height around 100 m that is detected before and after the morning rain shower.

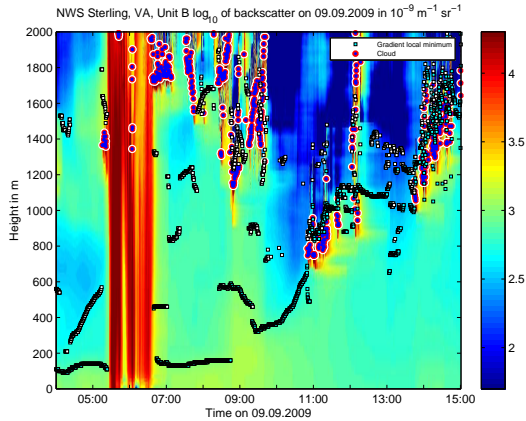


**Figure 5:** Overlap and range corrected ceilometer backscatter profiles recorded at the NWS test site Sterling, VA on September 9, 2009 treated with a cloud and precipitation filter and noise dependant averaging parameters.

The final step towards the enhanced gradient method involves the suppression of false layer hits generated by small fluctuations of the backscatter signal intensity. This is the case around 07:00 at heights between 400 m and 1000 m. Figure 6 shows a nocturnal layer followed by a convective layer with cloud formation raching 1600 m in the afternoon.

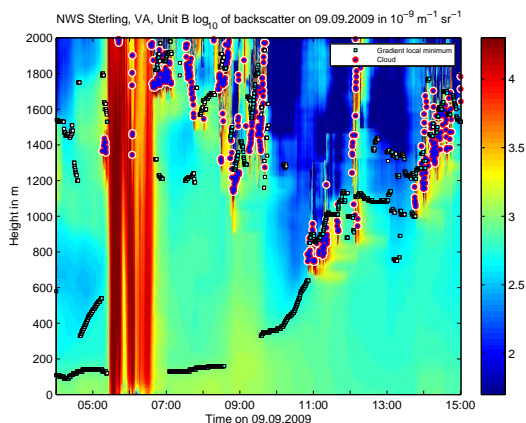


**Figure 6:** Final result of the enhanced gradient method applied to overlap and range corrected ceilometer backscatter profiles recorded at the NWS test site Sterling, VA on September 9, 2009.

#### 4. RESULTS

The enhanced gradient method introduced in the preceding section also sharpens the view on the cloudless day from Figure 1. In Figure 7, more near range details below 200 m can be seen, the false 500 m hits after 13:00 are suppressed, and the residual layer is detected until 08:00.

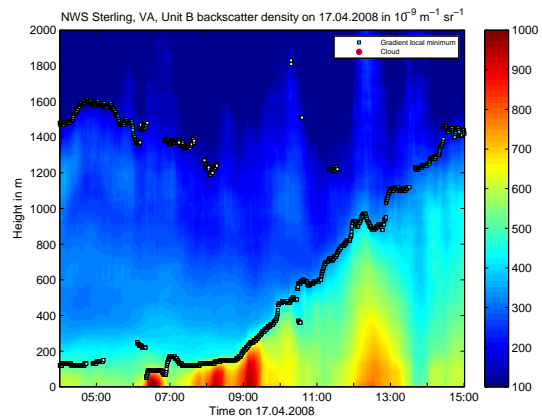


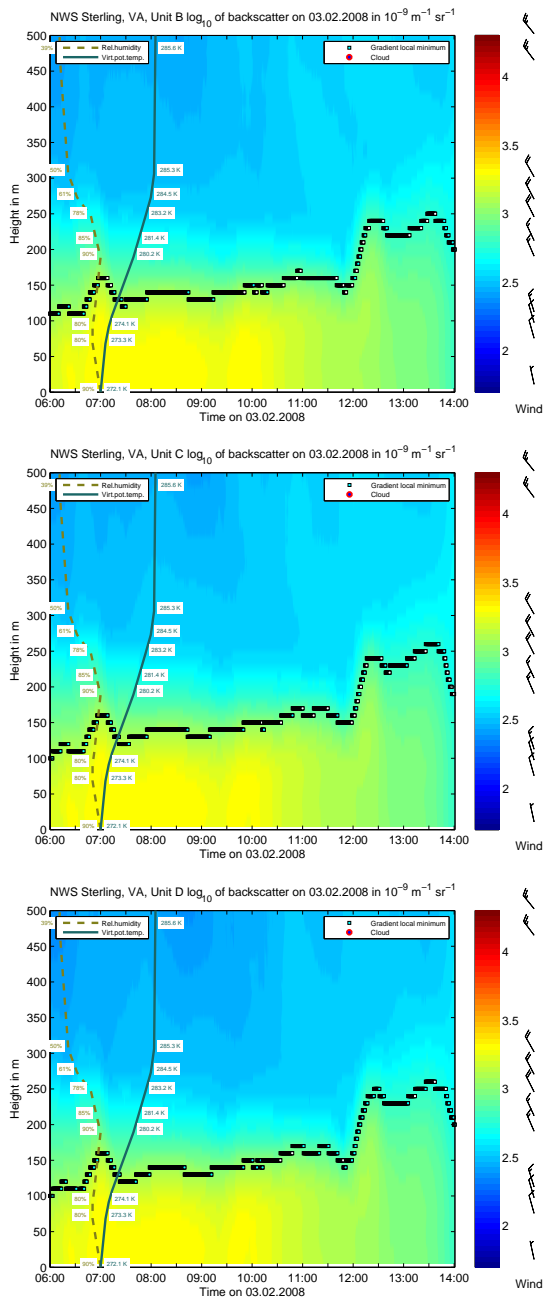
**Figure 7:** Density plot of overlap and range corrected ceilometer backscatter profiles recorded at the NWS test site Sterling, VA on April 17, 2008 and treated with the enhanced gradient method.

For nearly two years, the NWS has collected ceilometer backscatter profiles at its test site in Sterling, VA. During this period between three and six CL31 units had been operated in parallel.

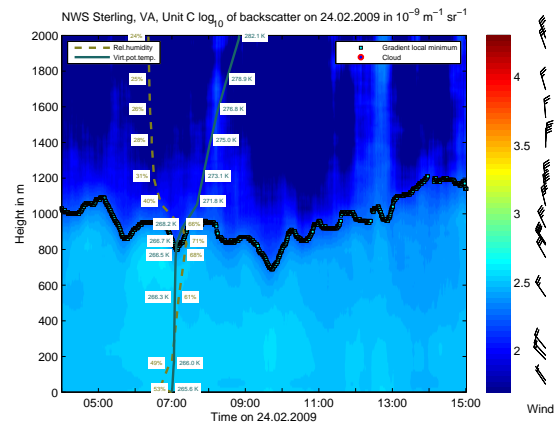
Regular sounding data from Sterling are available through the web site of the University of Wyoming (<http://weather.uwyo.edu/upperair/sounding.html>) that have been utilized for comparison in Figures 8 and 9.

Figure 8 shows a 150 m winter inversion layer detected by Sterling ceilometers that is confirmed by the virtual potential temperature profile from the 07:00 sounding. The three CL31 ceilometers operating in parallel do not only give the same aerosol layer height, but also report comparable backscatter amplitudes confirming the accuracy of the factory calibration procedure. A much higher reaching, but less dense winter aerosol layer that is also confirmed by virtual potential temperature profile and wind veering from northwest to north at the height of the inversion, is shown in Figure 9.

Several CL31 and CL51 ceilometers are operated in the Vaisala testfield in Helsinki, Finland. Their backscatter profiles can be compared to high resolution sounding data. The convective layer in Figure 10 is detected by both ceilometers and confirmed by the potential temperature profile. The improved signal-to-noise ratio of the CL51 reveals more details within and also above that layer.



**Figure 8:** Density plots of overlap and range corrected ceilometer backscatter profiles recorded by three co-located CL31 ceilometers at the NWS test site Sterling, VA on February 3, 2008. The virtual potential temperature profile from the Sterling sounding at 07:00 confirms the inversion layer height reported by the ceilometers. Wind barbs from the same sounding are given on the right side of the graph.



**Figure 9:** Density plot of overlap and range corrected ceilometer backscatter profiles recorded by a CL31 ceilometer at the NWS test site Sterling, VA on February 24, 2009. Relative humidity and virtual potential temperature profiles from the Sterling sounding at 07:00 confirm the inversion layer height reported by the ceilometer. Wind barbs from the same sounding show a veering wind at the same height.

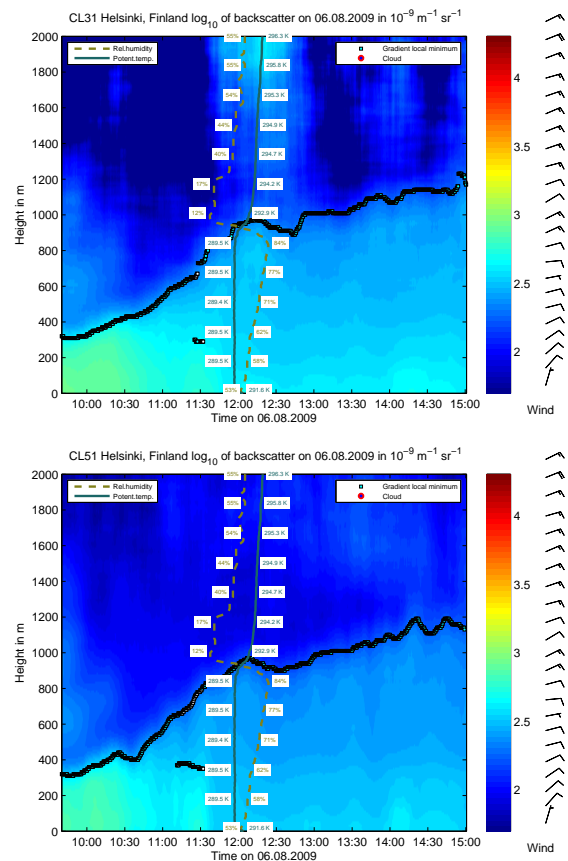


**Figure 10:** Density plots of overlap and range corrected ceilometer backscatter profiles recorded by a CL31 ceilometer (up) and a CL51 ceilometer at the Vaisala test site in Helsinki, Finland on August 6, 2009. The

potential temperature profile from a radiosonde launched at 12:03 at the same site confirms the height of a convective layer reported by both ceilometers. Wind barbs from the same sounding are given on the right side of the graph.

## 5. CONCLUSIONS AND OUTLOOK

Applying the enhanced gradient method introduced in this paper to a large variety of ceilometer profiles has confirmed its applicability for automatic boundary layer structure investigation.

It is currently integrated in the planetary boundary layer reporting and analysis tool Vaisala BL-VIEW. This supportive PC-software package is designed as a support and decision tool for air quality monitoring and research applications.

## 6. ACKNOWLEDGMENTS

The authors would like to thank the NWS for granting the permission to use the Sterling ceilometer test data for this publication.

## 7. REFERENCES

Emeis, S., K. Schäfer, C. Münkel, 2008: Surface-based remote sensing of the mixing-layer height – a review. - *Meteorol. Z.* **17**, 621-630.

[http://imk-ifu.fzk.de/downloads/Emeis\\_et\\_al\\_2008\\_Rem\\_Sensing\\_of\\_MLH\\_review.pdf?PHPSESSID=9sfvkvc00rdybfvceghd6mpc2](http://imk-ifu.fzk.de/downloads/Emeis_et_al_2008_Rem_Sensing_of_MLH_review.pdf?PHPSESSID=9sfvkvc00rdybfvceghd6mpc2)

Emeis, S., K. Schäfer, C. Münkel, 2009: Observation of the structure of the urban boundary layer with different ceilometers and validation by RASS data. - *Meteorol. Z.* **18**, 149-154.

[http://imk-ifu.fzk.de/downloads/Emeis\\_et\\_al\\_MetZet\\_2009\\_Ceilometer\\_RASS.pdf?PHPSESSID=p301qcn8c5svrtuldlc34qv7](http://imk-ifu.fzk.de/downloads/Emeis_et_al_MetZet_2009_Ceilometer_RASS.pdf?PHPSESSID=p301qcn8c5svrtuldlc34qv7)

Haman, C., B. L. Lefer, M. E. Taylor, G. Morris, B. Rappenglueck, 2010: Comparison of Mixing Heights using Radiosondes and the Vaisala CL31 Mixing Height Algorithm. - 15th Symposium on Meteorological Observation and Instrumentation at the 90th AMS Annual Meeting (Atlanta, GA).

[http://ams.confex.com/ams/90annual/techprogram/paper\\_165775.htm](http://ams.confex.com/ams/90annual/techprogram/paper_165775.htm)

Münkel, C., 2007: Mixing height determination with lidar ceilometers - results from Helsinki Testbed. - *Meteorol. Z.* **16**, 451-459.

Münkel, C., R. Roininen, 2008: Mixing layer height assessment with a compact lidar ceilometer. - Symposium on Recent Developments in Atmospheric Applications of Radar and Lidar at the 88th AMS Annual Meeting (New Orleans, LA).

<http://ams.confex.com/ams/pdfpapers/130028.pdf>

Münkel, C., S. Emeis, K. Schäfer, B. Brümmer, 2009: Improved near-range performance of a low-cost one lens lidar scanning the boundary layer. - In: Picard, R. H., K. Schäfer, A. Comeron, E. I. Kassianov, C. J. Mertens (Eds.): Remote Sensing

of Clouds and the Atmosphere XIV, Proc. SPIE, Bellingham, WA, USA, Vol. 7475.

Poyer, A. J., 2008: Evaluation of an MPL Cloud Detection Algorithm as a Reference for Ceilometer Testing Within the ASOS PI Program. - Symposium on Recent Developments in Atmospheric Applications of Radar and Lidar at the 88th AMS Annual Meeting (New Orleans, LA).

<http://ams.confex.com/ams/pdfpapers/130353.pdf>